Assignment of the Q_y Absorbance Bands of Photosystem II Chromophores by Low-Temperature Optical Spectroscopy of Wild-Type and Mutant Reaction Centers†

David H. Stewart,‡,§ Peter J. Nixon,|| Bruce A. Diner,⊥ and Gary W. Brudvig*,‡

Sterling Chemistry Laboratory, Yale University, P.O. Box 208107, New Haven, Connecticut 06520-8107, Central Research and Development Department, Experimental Station, E. I. du Pont de Nemours and Company, Wilmington, Delaware 19880, and Department of Biochemistry, Imperial College, London, SW7 2AY, United Kingdom

Received May 31, 2000

ABSTRACT: Photosystem II (PSII) contains a collection of pheophytins (Pheo) and chlorophylls (Chl) that have unique absorbance spectra depending on their electronic structure and the surrounding protein environment. Despite numerous efforts to identify the spectra of each cofactor, differing assignments of the chromophore absorbance bands and electrochromic effects have led to conflicting models of pigment organization and chromophore interactions in PSII. We have utilized low-temperature measurements on well-defined redox states, together with the use of site-directed mutants, to make spectral assignments of several reaction center (RC) chromophores. Cryogenic (77 K) optical spectroscopy has been used to trap the bound redox-active quinone, Q_A, in the reduced form and measure the effect of the redox state of Q_A on PSII chromophores without interference from other redox-active cofactors. The Q_A^- minus Q_A difference spectrum contains a number of features that represent the perturbation of Pheo and Chl absorbance bands upon Q_A reduction. Using site-directed mutants in which the axial ligand of the D1-side monomeric core Chl, P_A, is changed (D1-H198Q) or the hydrogen-bonding environment of the D1-side Pheo is modified (D1-Q130E), we have assigned the Q_y absorbance bands of four chromophores shifted by Q_A reduction including both RC Pheos, the D1-side monomeric accessory Chl (B_A), and one other Chl in PSII. The absorbance maximum of B_A was identified at 683.5 nm from least-squares fits of the D1-H198Q minus wild type (WT) Q_A^- minus Q_A double-difference spectrum; this assignment provides new evidence of a secondary effect of site-directed mutation on a RC chromophore. The other chromophores were assigned from simultaneous fits of the WT and D1-Q130E spectra in which the parameters of only the D1-side Pheo were allowed to vary. The D1-side and D2-side Pheos were found to have λ_{max} values at 685.6 and 669.3 nm, respectively, and another Chl influenced by Q_A^- was identified at 678.8 nm. These assignments are in good agreement with previous spectral analyses of intact PSII preparations and reveal that the number of chromophores affected by Q_A reduction has been underestimated previously. In addition, the assignments are generally consistent with chromophore positions that are similar in the PSII RC and the bacterial photosynthetic RC.

Photosystem II (PSII)[1] is a membrane-bound pigment−protein complex that converts light energy into chemical energy in order to oxidize H_2O to O_2. The minimal structure required for photochemistry—the reaction center (RC)—is comprised of the D1 and D2 polypeptides, cytochrome b_{559} (cyt b_{559}), and the PsbI protein and contains six chlorophyll (Chl) molecules and two pheophytin (Pheo) molecules (*1*−*6*). The PSII core complex includes the RC plus two Chl-binding proteins (CP43, CP47), extrinsic polypeptides bound outside the membrane, and several low molecular mass subunits (*7*). When illuminated with visible light, Chls in PSII absorb and transfer the light energy to a Chl molecule(s), P680, which initiates photochemistry (reviewed in ref *8*). The excited state of P680 (P680*) donates an electron to a

† This work was supported by Grant GM32715 (G.W.B.) from the National Institutes of Health, Grants 96-35306-3398 (G.W.B.) and 94-37306-0783 (B.A.D.) from the National Research Initiative Competitive Grants Program/USDA, by a National Institutes of Health predoctoral traineeship, GM08283 (D.H.S.), and The Royal Society and BBSRC (P.J.N.).

* To whom correspondence should be addressed. Telephone: (203)-432-5202. Fax: (203)432-6144. E-mail: gary.brudvig@yale.edu.

‡ Yale University.

§ Present address: Xanthon, Inc., P.O. Box 12296, Research Triangle Park, NC 27709.

|| Imperial College.

⊥ E. I. du Pont de Nemours and Company.

[1] Abbreviations: B_A/B_B, monomeric accessory Chls on the D1/D2 sides of PSII; BChl, bacteriochlorophyll; BPheo, bacteriopheophytin; BRC, non-sulfur purple bacterial photosynthetic reaction center; Car, redox-active carotenoid in PSII; Chl, chlorophyll; Chl_D, accessory Chl bound to D2-H117; Chl_Z, accessory Chl bound to D1-H118; CP43/CP47, Chl-binding proteins in PSII; cyt b_{559}, cytochrome b_{559}; D1/D2 polypeptides, reaction center polypeptides in PSII; EPR, electron paramagnetic resonance; LT, low temperature; L/M subunits, reaction center polypeptides in the BRC; MQ, menaquinone; P680, primary electron donor in PSII; P_A/P_B, monomeric reaction center core Chls on the D1/D2 sides of PSII; Pheo, pheophytin; PSI, photosystem I; PSII, photosystem II; Q_A/Q_B, redox-active quinones in PSII; RC, reaction center; RT, room temperature; WT, wild type; Y_Z/Y_D, redox-active tyrosines D1-Y161/D2-Y160 in PSII of *Synechocystis* PCC 6803.

10.1021/bi001246j CCC: $19.00
Published on Web 10/28/2000

Pheo acceptor to create a charge-separated state, $P680^+$-$Pheo^-$. The charge separation is stabilized on the acceptor side by electron transfer from $Pheo^-$ to a bound quinone, Q_A, and on the donor side by electron transfer from a redox-active tyrosine, Y_Z, to $P680^+$. Reduction of $Y_Z^\bullet$ is accomplished by a Mn_4 cluster that builds up oxidizing equivalents during subsequent charge separations in order to split H_2O. Q_A^- is oxidized by an exchangeable quinone that binds in a second quinone (Q_B) binding site.

Because the molecular structure of PSII has not been determined at the atomic level, structural considerations of PSII have been based on analogies to the crystal structure of the non-sulfur purple bacterial photosynthetic reaction center (BRC) (*9*−*11*). These comparisons are strongly supported by recent electron crystallography of the PSII CP47 RC at a resolution of 8 Å, which indicates that the positions of both the polypeptides and the chlorin cofactors of PSII are very similar to those in the BRC although the pair of core Chls analogous to the special pair bacteriochlorophyll (BChl) dimer are separated by a greater distance (∼11 Å versus 7.6 Å) (*12*). In addition, the BRC and the PSII RC are closely related by significant protein sequence similarity (reviewed in ref *9*), 2-fold symmetry (*9*, *10*, *13*, *14*), and similar electron-transfer pathways (*15*). For example, the two histidines in the L and M subunits of the BRC that bind the special pair BChl dimer (L-H173 and M-H200) are conserved in the D1 and D2 subunits of the PSII RC (D1-H198 and D2-H197) (*9*). In PSII, these histidines coordinate two core Chls, P_A and P_B, which are the likely site of P680 (*9*). Two other BChls are bound as monomeric accessory (voyeur) BChls and are ligated by L-H153 and M-H180 in the BRC (*16*). Although these histidines do not have direct homologues in the PSII RC (*9*), there are several potential Chl ligands in the D1 and D2 sequences that would allow binding of two voyeur-like Chls (B_A and B_B) in PSII (*14*), a scenario that is likely given the homology of the charge-separation reactions of the BRC and PSII (*17*). Because the BRC binds only four BChls and two bacteriopheophytins (BPheos), there are two Chls in the PSII RC that do not have homologues in the BRC. These Chls have been identified as the monomeric accessory Chls, Chl_Z and Chl_D, and are bound to histidines D1-H118 and D2-H117, which also lack homologues in the BRC (*14*).

The dense collection of chromophores and redox-active cofactors in the PSII RC creates an environment in which electron transfer through the protein can induce spectral shifts of some of the chromophores. This phenomenon of induced band shifts occurs in a manner that is dependent on the change in charge, the influence of this charge on the surrounding protein matrix, the dipole orientation and H-bonding of the oxidized/reduced cofactor and chromophores, and the spatial relationship of the chromophores relative to the oxidized/reduced cofactor (*18*). When the band shift is strictly the result of the chromophore interacting with a charged species, it is considered an electrochromic band shift and depends on the orientation of the chromophore, the distance between the charge and the chromophore, and the intervening dielectric of the protein medium between the charge and the chromophore (*19*). While redox-induced chromophore band shifts complicate the overall spectral properties of PSII, they can be exploited to obtain information about the identity of the individual chromophores. In particular, difference spectra can be used to great advantage to assign the spectra of individual chromophores contributing to the composite PSII spectrum.

Over the last three decades, there have been many studies aimed at identifying the Chls and Pheos in PSII and assigning the individual absorbance bands with which they are associated. Some approaches have utilized time resolution, chemical treatment, or LT to isolate and probe absorbance changes associated with different redox states of PSII. Several recent efforts include simulations of time-resolved $P680^+Pheo^-$/P680Pheo and $P680^+Q_A^-$/P680Q_A spectra (*20*, *21*), characterization of the effect of Pheo oxidation state on PSII spectra (*22*), and simulations of multiple time-resolved spectra from different redox changes in PSII to predict chromophore topology (*23*). Another strategy has been to utilize simulations of PSII spectra as a function of temperature in order to deconvolute the contribution from each chromophore (*24*). There have also been efforts to characterize PSII preparations in which the Chl content has been systematically changed by different detergent treatments or isolation procedures (*5*, *6*, *25*, *26*). While significant progress has been made, a consensus on definitive chromophore assignments remains elusive because of the spectral congestion in the PSII RC and the difficulty of preparing a sample with a well-defined, homogeneous redox state.

In this paper, we describe an alternative approach to assigning the absorbance bands of PSII chromophores that combines the use of site-directed mutants in which chromophore environments are perturbed with optical characterization of a well-defined redox state change of PSII. A series of mutations were made in close proximity to chromophores in the RC including the D1-side monomeric core Chl (P_A), the D1-side Pheo (Pheo(D1)), and the accessory Chls (Chl_Z and Chl_D). Utilizing a method for obtaining a Q_A^- minus Q_A spectrum free of interference from other redox changes, the spectral signatures of this redox state change were identified in the green and red wavelength regions in Mn-depleted PSII core complex preparations. In particular, this method of chemical treatment and LT trapping enabled isolation of the redox change of a single cofactor. Least-squares fits of the Q_A^- minus Q_A spectra were used to identify the features contributing to each spectrum, and assignments of the chromophores contributing to the spectra were made based on comparisons between mutant and wild-type (WT) spectra. Besides providing a specific probe of individual chromophores in the RC, this approach offers information about the topology of cofactors and chromophores in PSII. Insights obtained from this work are discussed in light of previous structural and spectroscopic chromophore assignments in PSII, as well as the BRC structure.

MATERIALS AND METHODS

Strains and Construction of Mutants. Site-directed mutations were introduced into a glucose-tolerant strain of the cyanobacterium, *Synechocystis* PCC 6803 (*27*). The D1-Q130E, D1-H198Q, and D1-H118Q/D2-H117Q mutants were prepared as described in refs *28*, *29* and *14*, respectively. All mutations were confirmed by sequencing PCR products amplified from fully segregated *Synechocystis* mutants.

PSII Isolation and Preparation. WT and mutant PSII core complexes comprising the D1 and D2 polypeptides, cyt b_{559},

CP47, CP43, and 33-kDa protein and containing about 40 Chl per PSII were purified from *Synechocystis* according to the method of Tang and Diner (*30*). Contaminating photosystem I (PSI) was at a low level as determined by electron paramagnetic resonance (EPR) and sodium dodecyl sulfate−polyacrylamide gel electrophoresis, and typical O_2-evolution rates were 2100−3200 μmol of O_2 (mg of Chl)$^{-1}$ h^{-1}. The core complexes were further simplified by removal of the Mn_4 cluster with 5 mM hydroxylamine treatment and washing with 5 mM ethylenediaminetetraacetic acid in pH 6.5 buffer (*31*). Chl *a* concentrations were determined by methanol extraction and using an extinction coefficient of 79.24 mL (mg of Chl)$^{-1}$ cm^{-1} at 665 nm (*32*). All protein purification and manipulation was carried out at 4 °C under dim green light. Sample concentrations were typically ∼150 μg of Chl/mL (∼4.4 μM PSII) for optical experiments and 0.27 mg of Chl/mL for EPR experiments.

Preparation of Redox States. Q_A^- was generated by room temperature (RT) illumination in the presence of the exogenous electron donor, NH_2OH, in a series of illuminations that allowed for the collection of spectra from PSII in several redox states. Prior to NH_2OH treatment and illumination, the PSII was dark-adapted on ice for ≥1 h to allow for dark reduction of $Y_D^\bullet$ (*33*, D. H. Stewart and G. W. Brudvig, unpublished results) so that the redox state of Y_D would not change during the course of the experiment due to slow reduction of $Y_D^\bullet$ by NH_2OH. Afterward, the PSII was dark-adapted on ice (3−5 min) with 1 equiv of $K_3Fe(CN)_6$ to oxidize dark-reduced Q_A and cyt b_{559} while avoiding a significant amount of residual oxidant, and then a 1000-fold excess of NH_2OH was added to the sample in the dark. Following the addition of NH_2OH, the sample was frozen to 77 K within 2 min to avoid chemical reduction of Q_A and cyt b_{559} by NH_2OH prior to collection of the nonilluminated scans. After collection of the nonilluminated scans at 77 K, the sample was illuminated at 77 K for 4−8 min to generate the $Chl_Z^+/Car^+/Q_A^-$ state, and 77 K illuminated scans were collected. Then the sample was thawed to RT in the dark over 2−3 min, allowing for reoxidation of Q_A by charge recombination. Next, the Q_A^- state was trapped by illuminating for 1 s at RT, dark adapting for 1 s at RT (to allow rereduction of Chl_Z^+, Car^+, and $Y_Z^\bullet$), and rapid freezing to 77 K in the dark. The freezing procedure involved immediately placing the sample in the cold vapor directly above (<1 cm) a liquid N_2 bath for 30 s and then gradually immersing the sample into the liquid N_2 over a 30-s period. After spectra of the RT illuminated sample were collected, the sample was illuminated for 4−8 min at 77 K, and 77 K illuminated spectra were collected to determine the amount of Q_A still oxidized after the RT illumination (see Results for an explanation of this analysis). In PSII core complexes, it is not necessary to add 3-(3,4-dichlorophenyl)-1,1-dimethylurea (DCMU) to block electron transfer beyond Q_A at RT because Q_B is absent from these preparations. The yields of Chl_Z^+/Car^+ and Q_A^- were measured by EPR and optical spectroscopy. The levels of $Y_D^\bullet$, $Y_Z^\bullet$, and $P700^+$ contamination in all of the difference spectra were less than 5%. All illuminations were performed using an Oriel quartz-halogen lamp (700 W/m^2). The cycle of freezing, thawing, and refreezing the sample had no effect on the absorbance spectrum of PSII in the absence of actinic illumination.

For comparison to the Q_A^- state, the charge separated state $Chl_Z^+/Car^+/Q_A^-$ was formed by continuous illumination of PSII with white light for 4−8 min (depending on the optical density of the sample) in a liquid nitrogen bath. Pretreatment with a 20-fold excess of $K_3Fe(CN)_6$ fully oxidized Q_A and cyt b_{559}, ensuring that all PSII centers were capable of forming reduced Q_A upon illumination and that Chl_Z^+/Car^+ would not be rereduced by cyt b_{559} during the illumination. For the purpose of EPR quantitation, $Y_D^\bullet$ minus Y_D (illuminated minus nonilluminated) difference spectra were produced by collecting nonilluminated scans of PSII that had been dark-adapted for ≥1.5 h in the absence of $K_3Fe(CN)_6$ and then dark-adapted for ≥30 min in the presence of a 20-fold excess of $K_3Fe(CN)_6$ (to allow for dark reduction of $Y_D^\bullet$ and then dark oxidation of Q_A^- and cyt b_{559}, respectively). Illuminated scans were collected after illumination at RT for 30 s, dark adaptation at RT for 30 s to allow for the rereduction of electron donors other than Y_D ($Y_Z^\bullet$, Chl_Z^+, and Car^+), and freezing to 77 K.

LT Optical Spectroscopy. Optical spectra were collected using a home-built Plexiglas flat cell submerged in a liquid N_2 bath in a quartz finger Dewar (Wilmad WG-850-B-Q). The flat cell had a ∼0.75 mm path length and a ∼45-μL sample volume. The unsilvered finger section of the Dewar was aligned in the sample beam of a Perkin-Elmer Lambda 6 or Lambda 20 UV−Vis spectrophotometer, and the flat cell was held in place by a plastic collar with a diameter slightly less than the inner diameter of the Dewar (∼5 mm). Interference from bubbles generated by liquid N_2 boil-off was avoided by careful cleaning of the Dewar with basic ethanol (0.125 g of KOH/mL) to limit nucleation sites on the quartz surface. Interference from frozen condensed moisture was minimized by maintaining a dry N_2 atmosphere above the Dewar. Before insertion into the finger Dewar, samples were frozen as uncracked glasses in the flat cell by rapid freezing (see previous section) in a liquid N_2 bath. 77 K actinic illumination of the optical samples was performed directly into the finger Dewar. Spectra were collected in two spectral windows (green and red wavelength regions) in order to maximize the signal-to-noise ratio in each window and to account for the different absorbance properties of PSII in each of the regions. No actinic effect was produced by the weak detecting beam of the spectrophotometer at 77 K as determined by a comparison of sequential scans of a nonilluminated sample to scans collected after 2 min of 77 K illumination with the quartz-halogen lamp; each of the sequential spectra was identical to the first nonilluminated scan and showed none of the light-induced features present in the scans collected after illumination.

Least-Squares Fitting of Optical Difference Spectra. The LT optical spectra were fit with a set of 2−8 Gaussian curves using a least-squares routine in Kaleidagraph version 3.0.9 graphics software. Each absorbance band was approximated by a single Gaussian line shape, and band shifts were generated from the difference between two Gaussians with equal bandwidths and amplitudes but different peak positions. All Chl absorbance amplitudes were fixed to the same value. Because of the smaller extinction coefficient of Pheo relative to Chl (*20*, *32*, *34*), Gaussian line shapes used to model Pheos were normalized by 0.6 relative to the Gaussian line shapes that represented Chls. Fits were performed on spectra plotted as a function of energy (cm^{-1}). However, analogous fits of

spectra plotted as a function of wavelength showed that the wavelength-dependent compression of absorbance bands was insignificant over the narrow range examined (650−700 nm); therefore, all spectra are presented as a function of wavelength. To obtain fits for WT and mutant spectra simultaneously, a least-squares routine was run for each spectrum in which all of the band shifts were fixed except one which represented the chromophore that was perturbed by the mutation. To determine the positions of other chromophores, their band shifts were shifted the same amount for both spectra in an iterative manner until the best fits were obtained.

While the least-squares fits provided very good simulations of the experimental spectra, there are several factors not modeled by the fits that may account for the minor differences between the experimental and simulated spectra. The simulated absorbance bands in this study were approximated as Gaussian line shapes. This assumption ignores vibrational transitions that broaden absorbance bands toward higher energies. Although vibronic structure may have a small effect on the peak positions of the PSII chromophores, including it in the fits would have introduced an additional set of unknown parameters. In addition, in comparing WT and the D1-Q130E mutant, the bandwidth and λ_{max} were allowed to vary for only a single chromophore in each spectrum: the chromophore most directly affected by the mutation. This approach avoided the introduction of spectral variation lacking a known structural precedent and is supported by the assertion that Chl spectral heterogeneity is due primarily to local differences in protein environment (*35*, *36*).

LT EPR. Cryogenic EPR spectra were collected on a Varian E-line EPR spectrometer equipped with an Oxford Instruments ESR 900 liquid helium cryostat. Spectrometer conditions were as follows: microwave frequency, 9.28 GHz; microwave power, 0.03 mW (Chl_Z^+/Car^+ and $Y_D^\bullet$) or 20 mW (Q_A^-); magnetic field modulation amplitude, 2 G (Chl_Z^+/Car^+ and $Y_D^\bullet$) or 20 G (Q_A^-); temperature, 30.0 K (Chl_Z^+/Car^+ and $Y_D^\bullet$) or 5.9 K (Q_A^-). The Chl_Z^+/Car^+ and $Y_D^\bullet$ signals were collected under nonsaturating conditions. Fremy's salt was used as a standard for spin quantitation (*37*).

RESULTS

To characterize the effect of a negative charge on Q_A^-, LT optical spectra of $NH_2OH/K_3Fe(CN)_6$-treated PSII were collected before and after RT illumination. Difference spectra were obtained throughout the visible wavelength range. Results from the green and red regions are shown in Figure 1. The red wavelength region was particularly rich with absorbance signals revealing two or more band shifts in the Q_y region. Absorbance changes in the difference spectrum of the Q_y region were approximately 20−50 times smaller than the absorbance maximum of the Q_y band, which represents a superposition of all of the neutral Chls and Pheos in PSII. This ratio is reasonable considering that there are about 40 Chls and 2 Pheos per PSII core complex (*30*). No signals were observed in difference spectra of the Chl Q_x region, probably because they were too small relative to the noise to be detected in these experiments. However, a flat baseline in difference spectra of the Q_x region provided an indication of a good subtraction in both the Q_x region and the Q_y region. No Q_y absorbance bands were expected to be enhanced or bleached (only shifted) as a result of Q_A reduction, so the Q_A^-/Q_A subtraction was performed such that the integrated area under the difference spectrum in the Q_y region was zero.

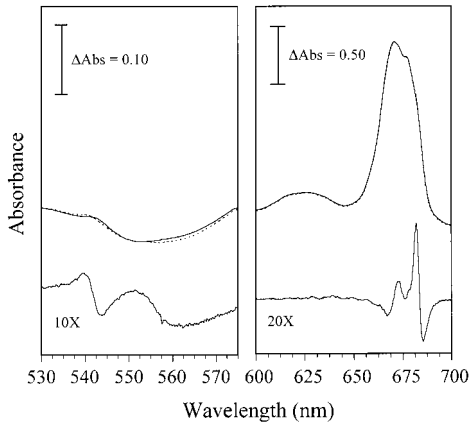

FIGURE 1: Low-temperature optical spectra of $NH_2OH/K_3Fe(CN)_6$-treated WT PSII. The left and right panels show the green and red wavelength regions, respectively (note the different abscissa scales). The top two traces in each panel are RT illuminated (—) and nonilluminated (- - -) scans; the bottom traces are the illuminated minus nonilluminated difference spectra magnified 10- or 20-fold (—).

Table 1: Summary of Signal Yields in Optical and EPR Difference Spectra of PSII Core Complexes Treated with 1 Equiv of $K_3Fe(CN)_6$ and then 1000 Equiv of NH_2OH

	EPR signal area[a]			optical signal height[b]
difference spectrum	Q_A^-	Chl_Z^+/Car^+	$Y_D^\bullet/Y_Z^\bullet$	Q_A^-
RT *hν* minus dark	74	<3	0	90
RT *hν*/77 K *hν* minus RT *hν*	<12	23	<3	10
77 K *hν* minus dark	80	81	<10	79

[a] The Q_A^- EPR signal areas are reported as a percentage relative to the integrated area of Q_A^- after 77 K illumination and RT illumination. The Chl_Z^+/Car^+ and $Y_D^\bullet$ EPR signal areas are relative to the double integrated area of the full yield of $Y_D^\bullet$ produced in a sample with matched concentration (see Materials and Methods). The values of percent change in EPR signal areas have an uncertainty of ±10 for Q_A^- and ±5 for Chl_Z^+/Car^+ and $Y_D^\bullet$. [b] The Q_A^- optical signal heights are reported as a percentage relative to the peak-to-trough height of the C550 signal in the 77 K illuminated and RT illuminated minus dark difference spectrum. The values of percent change in optical signal height have an uncertainty of ±10.

The amount of Q_A^- trapped by the RT illumination protocol was quantified on the basis of the C550 signal in the illuminated minus nonilluminated difference spectrum in the green wavelength region (Table 1). This derivative-shaped feature with λ_{max} = 540 nm and λ_{min} = 544 nm (sharpened at 77 K relative to RT) has been assigned previously as an electrochromic shift of the Pheo absorbance band caused by a perturbation of its local electric field due to the change in redox state of Q_A^- (*38*, *39*). In addition, the absence of any signal at 559 nm indicates that the redox state of cyt b_{559} was not changed by RT illumination. In general, the red wavelength region contained the sharpest and most well-resolved features in the Q_A^- minus Q_A spectrum. Furthermore, its spectral complexity indicated the contribution of multiple chromophores. Therefore, we have focused on the Q_A^- minus Q_A difference spectrum in the Q_y region as the subject of this paper.

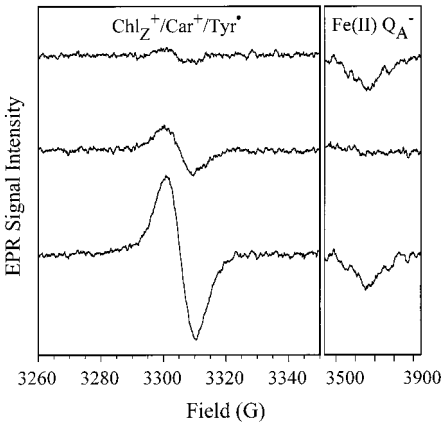

FIGURE 2: Low-temperature EPR difference spectra of $NH_2OH/K_3Fe(CN)_6$-treated WT PSII showing the $Chl_Z^+/Car^+/Tyr^\bullet$ (left panel) and Fe(II)Q_A^- (right panel) signals. The difference spectra are plotted as follows: RT illuminated minus nonilluminated (top trace), RT and 77 K illuminated minus RT illuminated (middle trace), and 77 K illuminated minus nonilluminated (bottom trace).

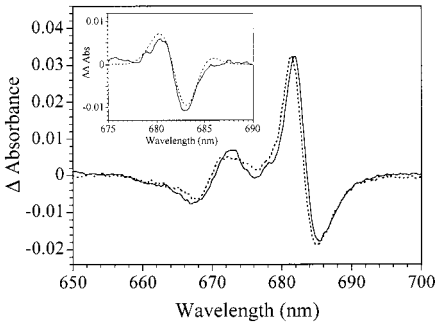

FIGURE 3: Low-temperature optical difference spectra of $NH_2OH/K_3Fe(CN)_6$-treated WT (—) and D1-H198Q (- - -) PSII in the red wavelength region. The spectra are RT illuminated minus nonilluminated difference spectra. Inset: The double-difference spectrum of D1-H198Q minus WT (—) and the least-squares fit of the double-difference spectrum (- - -).

The yields of Q_A^- as well as Chl_Z^+/Car^+, $Y_D^\bullet$, and $Y_Z^\bullet$ were confirmed by LT EPR spectroscopy (Figure 2, Table 1). The left panel of Figure 2 shows the $g = 2$ region of the EPR spectrum in which oxidized Chl, Car, and tyrosine can be detected, and the right panel shows the $g = 1.83$ region where a signal from reduced Q_A (Fe(II)Q_A^-) can be detected (*40*). A significant yield of Q_A^- is present only in the first and third traces. There is essentially no contribution (<3% of centers) from Chl_Z^+/Car^+, $Y_D^\bullet$, or $Y_Z^\bullet$ in the Q_A^- minus Q_A spectrum (top trace). In addition, the yield of Q_A^- following RT illumination is nearly the same as that obtained by 77 K illumination alone (bottom trace). The RT/77 K illuminated minus RT illuminated spectra (middle traces) show the signals induced by 77 K illumination of the sample already illuminated at RT. These spectra reflect the number of centers that still contained oxidized Q_A (and were still capable of charge separation) after the RT illumination. Thus, the small Chl_Z^+/Car^+ signal and negligible Fe(II) Q_A^- signal indicate that only a small amount of Q_A (~10−20%) remained oxidized after the RT illumination.

To assign the individual chromophores contributing to the Q_A^- minus Q_A spectrum, several site-directed mutants were compared to WT. A Q_A^- minus Q_A spectrum was obtained for D1-H198Q (Figure 3), and a direct comparison to WT was made by generating a double-difference spectrum (inset Figure 3). The fact that there is a feature in the double-difference spectrum indicates that the D1-H198Q mutation perturbs the Q_y band of one of the chromophores in PSII and, more importantly, that the absorbance band of this chromophore is shifted by the reduction of Q_A. The observation of a spectral shift in the Q_y region of D1-H198Q relative to WT is consistent with previous studies on this same mutant which show a perturbation of the WT spectrum of P_A in both the Soret and Q_y regions although the major change observed in the Q_y region is a band shift from 672 to 669 nm (Diner, B. A., Nixon, P. J., Coleman, W. J., Schlodder, E., Rappaport, F., Lavergne, J., and Chisholm, D. A., manuscript in preparation). The difference between the Q_A^- minus Q_A spectrum of WT and D1-H198Q was confirmed by $Chl_Z^+/Car^+/Q_A^-$ minus $Chl_Z/Car/Q_A$ spectra which are also different in D1-H198Q relative to WT (data not shown). These latter spectra are not included in this paper because they contain contributions from at least three charged species and reflect electrostatic influences from cofactors on both the acceptor and donor sides of PSII. Although it appears that there is also a small shift at ~670 nm in the Q_A^- minus Q_A spectrum of D1-H198Q as compared to WT, this represents spectral variation rather than a real mutation-induced shift as evidenced by the absence of well-defined band shifts in the double-difference spectrum.

If the D1-H198Q mutation shifts the absorbance of a chromophore in only one of the Q_A redox states (reduced or oxidized), then the double-difference spectrum would take the shape of a symmetric Gaussian first-derivative-shaped feature. On the other hand, if the D1-H198Q mutation influences a chromophore in both Q_A redox states, then the double-difference spectrum would represent a shift of a band shift—giving a feature with three components (Gaussian second-derivative-shaped feature) with the symmetry of the feature depending on the relative sizes of the mutation-induced shifts in each of the redox states of Q_A. Clearly, the D1-H198Q minus WT double-difference spectrum is asymmetric, resembling the latter of these cases more closely. (Here, we make the simplifying assumption that the mutation affects only a single chromophore.) Consequently, it was best fit as the difference of two band shifts, each having different shift magnitudes (inset of Figure 3). The parameters obtained from this fit provide an approximate bandwidth for one of the RC Chls in PSII and also define the positions of its absorbance band in both Q_A redox states for WT and D1-H198Q. From this analysis, it was determined that in WT PSII a Chl with a bandwidth ~4 nm absorbs at 683.5 nm when Q_A is oxidized and shifts to 682.8 nm upon Q_A reduction. In the D1-H198Q mutant, these positions are 682.8 and 681.6 nm, respectively. In the above analysis, we considered all of the RC chromophores as monomeric species with no significant electronic coupling among chromophores. This approximation enabled us to eliminate the effect of exciton coupling on the chromophore positions and intensities. While the extent of chromophore coupling within the PSII RC is still currently under debate, there is ample experimental evidence supporting a weak coupling model (see ref *20* and references therein).

Additional information about the chromophores contributing to the Q_A^- minus Q_A spectrum was obtained from a comparison of the Q_A^- minus Q_A spectra for WT and the mutant, D1-Q130E (Figure 4). The glutamine at position

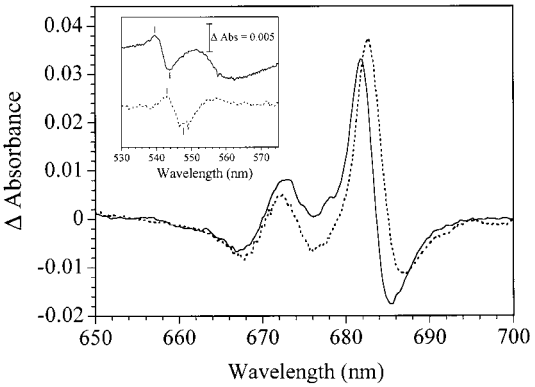

FIGURE 4: Low-temperature optical difference spectra of NH_2OH/$K_3Fe(CN)_6$-treated WT (—) and D1-Q130E (- - -) PSII in the red wavelength region. The spectra are RT illuminated minus nonilluminated difference spectra. Inset: Same difference spectra in the green wavelength region.

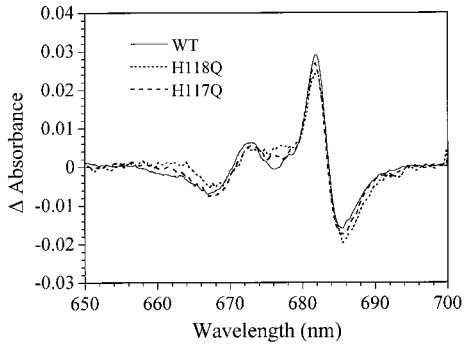

FIGURE 5: Low-temperature optical difference spectra of NH_2OH/$K_3Fe(CN)_6$-treated WT (—), D1-H118Q (- - -), and D2-H117Q (— —) PSII in the red wavelength region. The spectra are RT illuminated minus nonilluminated difference spectra.

D1−130 in WT is closely associated with the active (D1) Pheo of PSII in an interaction which is modified by replacement of the native residue with glutamic acid (*28*). The difference between the Q_A^- minus Q_A spectra for WT and D1-Q130E is significantly larger than that seen for WT versus D1-H198Q indicating that the Q_y absorbance band of the D1-side Pheo is shifted by Q_A reduction and also by the D1-Q130E mutation. Furthermore, the C550 signal associated with this Pheo is red-shifted by ∼2.5 nm in D1-Q130E relative to WT (inset of Figure 4), consistent with Pheo Q_x band bleaching experiments in PSII (*28*), optical measurements of L-branch BPheo mutants in the BRC (*41*), and assignment of the C550 signal as originating from Pheo (*38*, *39*). A similar shift of the Pheo Q_x absorbance band also has been observed at RT (Force, D. A., Nixon, P. J., and Diner, B. A., unpublished results). The broad negative feature at ∼562 nm that appears in the WT spectrum (Figure 4, inset) is not a consequence of Q_A reduction; rather, it represents a baseline artifact.

The assignment of chromophores contributing to the Q_A^- minus Q_A spectrum was supported by analysis of Q_A^- minus Q_A spectra collected from two other mutants, D1-H118Q and D2-H117Q (Figure 5). D1-H118 and D2-H117 are the respective axial histidine ligands of the accessory Chls, Chl_Z and Chl_D. Both of these mutants have spectra identical to WT, a characteristic that is consistent with the interpretation that neither of the absorbance bands of Chl_Z or Chl_D is influenced by the redox state of Q_A.

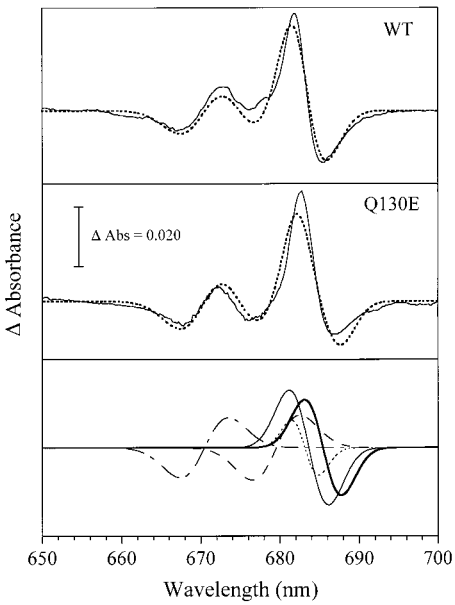

FIGURE 6: Four-chromophore fits of absorbance changes induced by Q_A reduction in WT (top panel) and D1-Q130E (middle panel) PSII. The top two panels show the experimental spectra (—) and the least-squares fits (- - -), and the bottom panel shows the individual band shifts that comprise the least-squares fits. The band shifts for Pheo(D2) (- — -), B_A (•••), and Chl (— —) are the same for WT and Q130E; the band shift for Pheo(D1) is different for WT (thin solid line) relative to D1-Q130E (bold solid line).

Because of the more complicated nature of the mutation-induced shifts in the Q_A^- minus Q_A spectrum, the WT and D1-Q130E spectra were fit simultaneously instead of fitting the double-difference spectrum. This strategy of global analysis decreases the number of independent parameters per data set (spectrum), thereby increasing the accuracy and confidence in each parameter (*24*). In addition, this approach allowed for the assignment of another chromophore that contributes to the Q_A^- minus Q_A spectrum besides Pheo(D1). Figure 6 shows the experimental spectrum and the best fit for WT (top panel) and D1-Q130E (middle panel) PSII; the bottom panel displays the individual band shifts which, when summed, give the spectral fits.

The procedure for assigning chromophores in PSII based on Q_A^- minus Q_A difference spectra was as follows. (i) The position and bandwidth of one Chl was determined from the least-squares fit of the H198Q minus WT Q_A^- minus Q_A double-difference spectrum (see above). (ii) The isolated band shift centered at ∼670 nm was fit as the difference of two Gaussians with a bandwidth of 7 nm and positions of 669.3 and 671.6 nm when Q_A is oxidized and reduced, respectively. The chromophore responsible for this band shift was assigned as the inactive (D2) Pheo based on a previous identification of the inactive Pheo absorbance band at ∼670 nm (*22*), the lack of any difference between WT and D1-Q130E in this region of the spectrum, and the close proximity of Pheo(D2) to Q_A. (iii) The Chl and Pheo(D2) positions and bandwidths were fixed, and the rest of the spectrum from 650 to 700 nm was simultaneously fit for WT and D1-Q130E to 1, 2, or 3 band shifts. During the least-squares fitting procedure, only one band shift was allowed to differ between D1-Q130E and WT corresponding to the absorbance band of Pheo(D1). After obtaining the best fits of the Q_A^- minus Q_A spectra, it was determined that fits with a *total* of 3 band shifts did not reproduce the experimental spectrum as well

Table 2: Summary of Absorbance Band Parameters for WT PSII Assigned from Four-Chromophore Least-Squares Fits of Q_A^- Minus Q_A Difference Spectra from WT and Mutant PSII

chromophore	λ_{max} (nm) (Q_A/Q_A^-)	bandwidth (fwhm, nm)
active Pheo(D1)	685.6/681.7 (±0.2)	5
inactive Pheo(D2)	669.3/671.6 (±0.3)	7
B_A Chl	683.5[b]/682.8 (±0.1)	4
Chl[a]	678.8/680.2 (±0.3)	7
Chl_Z	not shifted by Q_A^-	
Chl_D	not shifted by Q_A^-	
P_A Chl	672[b]/−; not shifted by Q_A^-	
P_B Chl	not shifted by Q_A^-	

[a] Tentatively assigned as B_B Chl. [b] Diner, B. A., Nixon, P. J., Coleman, W. J., Schlodder, E., Rappaport, F., Lavergne, J., and Chisholm, D. A., manuscript in preparation.

as the 4-band shift fits and that fits with 5 band shifts did not reach a local minimum, indicating that 5 band shift fits contain too many parameters to be constrained by the available data. The 4-band shift fits showed a good resemblance to the experimental spectra and could be justified based on analogy to the BRC structure (Table 2). This result indicates that besides a Chl, Pheo(D2), and Pheo(D1), an additional Chl is influenced by Q_A reduction.

The additional Chl identified from the 4-chromophore fits was assigned a bandwidth of 7 nm. This bandwidth is within the range of values determined from other LT absorbance spectra (*20*, *21*, *42*, *43*) and simplified our fits by reducing the number of variables. The individual Chl absorbance maximum obtained from the 4-chromophore fit is ∼0.03 absorbance units, a value that is in agreement with the overall Q_y absorbance maximum of the PSII sample (∼1.3) considering about 40 overlapping Chls per PSII complex. The spectral parameters and chromophore assignments obtained from the fits of WT and D1-Q130E are summarized in Table 2.

Of the two Pheos and two Chls comprising the Q_A^- minus Q_A fits, each chromophore type has one blue-shifting and one red-shifting band. The red-shifting chromophores are the 7 nm bandwidth Chl and Pheo(D2), and the blue-shifting chromophores are the Chl identified from the WT/D1-H198Q comparison and Pheo(D1). The dominant band shift in both WT and D1-Q130E spectra is the chromophore affected by the D1-Q130E mutation, Pheo(D1). When Q_A is oxidized, the Pheo(D1) absorbance band is at 685.6 nm (WT) or 686.9 nm (D1-Q130E), and when Q_A is reduced the Pheo(D1) band is blue-shifted by 3.9 nm in WT and 2.9 nm in D1-Q130E. Thus, the effect of the D1-Q130E mutation on the Q_A^- minus Q_A spectrum is a red-shift of the Pheo(D1) absorbance band and a slight decrease in the intensity of the Pheo(D1) band shift.

DISCUSSION

The spectra presented in this paper combine the advantages of LT measurement of well-defined charge-separated states and site-directed mutation to provide detailed information about individual chromophores in PSII. The use of intact PSII core complexes purified by mild detergent extraction (*30*) in this study ensured minimal perturbation of the RC and its chromophores during the isolation procedure. Chemical treatment and 77 K measurement enabled us to trap a well-defined redox state change for the bound quinone, Q_A.

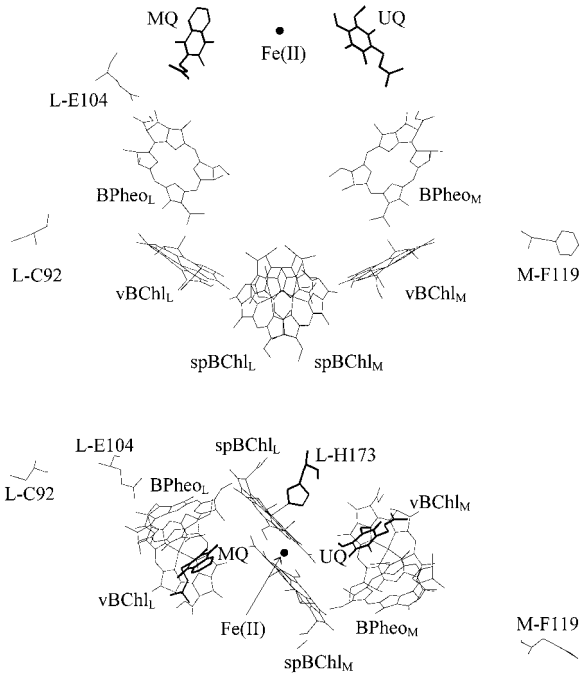

FIGURE 7: Top: Side-on view (in the membrane plane). Bottom: Stromal-side view (along the membrane normal) of the chromophores and relevant amino acids in the BRC from *R. viridis* (*44*). The chromophores are indicated as follows: L and M branch special pair BChls (spBChl$_L$, spBChl$_M$), L and M branch monomeric "voyeur" BChls (vBChl$_L$, vBChl$_M$), L and M branch BPheos (BPheo$_L$, BPheo$_M$), ubiquinone (UQ, analogous to Q_B), menaquinone (MQ, analogous to Q_A), and the non-heme Fe(II) atom (Fe(II)). The amino acids are L-C92 (the homologue of D1-H118, the axial ligand to Chl_Z), M-F119 (the homologue of D2-H117, the axial ligand to Chl_D), L-E104 (the homologue of D1-Q130E), and L-H173 (the homologue of D1-H198).

In addition, individual chromophore absorbance bands are narrower at lower temperatures (*24*), making them more readily resolved. Previous studies of the $P680^+$-Q_A^- state have shown that spectral resolution of 77 K absorbance spectra is significantly improved over RT spectra as a consequence of this spectral narrowing (*21*).

Relevance of the Bacterial Reaction Center Structure. In evaluating the least-squares fits of the Q_A^- minus Q_A difference spectra and assigning deconvoluted absorbance bands to specific chromophores, it is extremely useful to take advantage of the known structural similarity between the BRC and PSII. We used the crystal structure of the BRC from *R. viridis* (*44*) (PDB 1PRC) as a template for assessing the likelihood of electrochromic interactions in PSII. Two views of the BRC chromophores including the special pair BChl dimer, the voyeur accessory BChls, the BPheos, and the Q_A and Q_B homologues (menaquinone (MQ) and ubiquinone, respectively) are presented in Figure 7. In both views, three BRC amino acids are highlighted because of the relevance of their PSII homologues: L-C92 and M-F119 are homologous to D1-H118 and D2-H117, respectively (*14*), and L-E104 is homologous to D1-Q130. The stromal side view also shows L-H173, the homologue of D1-H198. To aid in the comparison of charge−chromophore interactions, the center-to-center distances between MQ and each of the BRC chromophores and the angles between MQ and the *y*- and *x*-axes of the BRC chromophores were estimated from the BRC coordinates; the values are summarized in Table 3.

Table 3: Summary of Distances (Å) and Orientations of Menaquinone (MQ) Relative to Each of the Chromophores in the BRC Measured from the 2.30-Å Crystal Structure of *R. viridis* (PDB 1PRC)[a]

chromophore	distance from MQ (Q_A)[b]	orientation with respect to *y*-axis[g] (deg)	orientation with respect to *x*-axis[g] (deg)	predicted shift of Q_y by Q_A^- [i]
special pair BChl (L)[c]	28.0	−74	+27	blue
special pair BChl (M)[c]	28.3	−56	+34	blue
voyeur BChl (L)[c]	23.8	−72	+68	blue
voyeur BChl (M)[c]	30.0	+79	−88	red
BPheo (L)[d]	14.4	+47	+82	red
BPheo (M)[d]	23.3	+60	−55	red
L-C92 [Chl_Z][e]	32.8	NA	NA	NA
M-F119 [Chl_D][f]	42.0	NA	NA	NA

[a] For comparison to PSII: MQ corresponds to Q_A, L-C92 is homologous to D1-H118, M-F119 is homologous to D2-H117, L-E104 is homologous to D1-Q130E, and L-H173 is homologous to D1-H198. [b] Distances were calculated from the center of the MQ ring by averaging the distances to three nonadjacent carbons in the ring. [c] Distances were measured from the magnesium in the center of the BChl rings. [d] Distances were estimated to the center of the BPheo macrocycles by averaging the distances to the four pyrrole nitrogens. [e] Distances were estimated to the center of the Chl_Z macrocycle by using the sulfur atom of L-C92, which is expected to be in a comparable position to the nitrogen of D1-H118 that serves as the axial ligand to Chl_Z. [f] Distances were estimated to the center of the Chl_D macrocycle by using the average of the distances to the C3 and C5 positions of the phenylalanine ring of M-F119. These carbon atoms, four atoms away from the protein backbone, are expected to be in comparable positions to the nitrogen of D2-H117, which serves as the axial ligand to Chl_D. [g] Angles were measured between the center of MQ ring[b] and the *y*-axis or *x*-axis of each chromophore[h] using the center of the BChl or BPheo ring as the vertex of the angle. Orientations of the *y*-axis in which Q_A was closer to ring III and orientations of the *x*-axis in which Q_A was closer to ring IV were arbitrarily assigned as positive angles. [h] The *y*-axis was approximated as a vector between the pyrrole nitrogens of rings I and III, and the *x*-axis was approximated as a vector between the pyrrole nitrogens of rings II and IV. [i] The predicted Q_y band shift directions were determined using the measured orientation of MQ relative to the *y*-axis of each chromophore as described in ref *19*. A positive angle indicates that MQ is closer to ring III, and a negative angle indicates that MQ is closer to ring I.

Chromophore Assignments. The comparison of Q_A^- minus Q_A spectra lacking contributions from oxidized electron donors for WT and several site-directed mutants of PSII makes possible a straightforward identification of chromophores that are influenced by the redox state of Q_A. Specifically, at least one Chl and one Pheo are influenced by the negative charge on Q_A as evidenced by mutation-induced shifts of their absorbance bands in Q_A^- minus Q_A spectra of D1-H198Q and D1-Q130E. In the case of the Chl, the shift induced by the D1-H198Q mutation is a subtle change from the WT Q_A^- minus Q_A spectrum, but the perturbation is readily apparent in the double-difference spectrum. The double-difference spectrum is an isolated representation of the effect of the mutation on the response of this Chl to the redox state of Q_A; as such, this spectrum contains information about the position and shape of the Chl absorbance band that can be extracted from least-squares fits of the spectrum.

Because the D1-H198Q mutation replaces a histidine that is homologous to the axial ligand of the L-branch special pair BChl, the expected identity of the Chl influenced by this mutation is the D1-side monomeric core Chl, P_A. Recent LT (5 and 120 K) optical experiments examining $P680^+$ minus P680 spectra and $^3P680$ minus P680 spectra for WT and D1-H198Q have supported this expectation by revealing a ~3 nm blue shift of the P_A absorbance band in D1-H198Q (669 nm) relative to WT (672 nm) (Diner, B. A., Nixon, P. J., Coleman, W. J., Schlodder, E., Rappaport, F., Lavergne, J., and Chisholm, D. A., manuscript in preparation). However, the Q_A^- minus Q_A spectra presented here show a very small shift associated with the D1-H198Q mutation (~0.7 nm). In addition, the λ_{max} of the Chl that is affected by both D1-H198Q mutation and Q_A reduction is 683.5 nm rather than 672 nm. These observations, along with the large distance expected between Q_A and P_A based on BRC homology (28.0 Å, Table 3), argue against the assignment of the 683.5 nm Chl as P_A. Interestingly, the aforementioned studies of Diner et al. have identified a second Chl associated with the absorbance spectrum of $^3P680$ and P_A that absorbs at 682−684 nm and is assigned to the D1-side monomeric accessory Chl, B_A. Because of the closer proximity of the L-branch voyeur BChl to MQ, the previous assignment of B_A at 682−684 nm, and the observation that B_A is associated with P_A, we assign B_A as the ~4-nm-wide absorbance band that absorbs at 683.5 nm when Q_A is oxidized.

The assignment of B_A based on changes induced by the D1-H198Q mutation requires that there is a secondary effect of this mutation on the B_A Chl in addition to the effect on the P_A Chl which is directly ligated by D1-H198. There are at least two possibilities that can explain this observation. One explanation is that the P680 Chls are excitonically coupled such that there is overlap between the electronic transitions of P_A and B_A. If this is the case, then the absorbance profile of both chromophores would be expected to be perturbed by the D1-H198Q mutation, although the extent to which B_A is affected would depend on the strength of the exciton coupling. Alternatively, the secondary effect of the mutation on B_A may be a consequence of structural perturbation of the protein that affects not only P_A but also B_A, leading to a large shift of the P_A absorbance band and a small shift of the B_A absorbance band.

The fact that the D1-Q130E mutation changes the Q_y band in the Q_A^- minus Q_A spectrum relative to WT confirms that Pheo(D1) is affected by the reduction of Q_A. Giorgi et al. showed that the D1-Q130E mutation affects the Pheo(D1) Q_x absorbance band via a 2.5-nm red shift (*28*), and this Pheo is expected to be very close to Q_A (Table 3) so the interaction between Q_A^- and Pheo(D1) is not surprising. By utilizing simultaneous least-squares fits of WT and D1-Q130E Q_A^- minus Q_A spectra and including the parameters obtained for B_A and Pheo(D2), we were able to identify and assign the absorbance bands of Pheo(D1) and another Chl associated with the PSII RC (Table 2). Our spectral analysis shows that the mutation-induced red shift of the Pheo(D1) Q_x band is paralleled by a red shift of the Q_y band. The difference between the Pheo(D1) absorbance band in WT versus D1-Q130E may represent a subtle change in the electronic environment around Pheo(D1) caused by the mutation. The Q to E mutation probably changes the hydrogen-bonding interaction between the D1−130 amino acid and Pheo(D1). Both of these factors would be expected to influence the interaction of Pheo(D1) with Q_A in its oxidized and reduced forms. This phenomenon reflects an interesting electronic and/or structural modification of PSII that is relevant to the

efficiency of charge separation (*28*) and requires further study.

The fourth chromophore that is perturbed by a negative charge on Q_A is a red-shifting Chl absorbing at 678.8 nm. The possible assignments for this Chl are the remaining Chls in the PSII RC core [P_A, P_B, B_B, Chl_Z, or Chl_D] or an additional Chl at the perimeter of the D1/D2 complex in close enough proximity to Q_A to be influenced by Q_A reduction. The identity of the 678.8-nm Chl is not likely to be a Chl in CP47 based on the positions of the CP47 Chl electron densities assigned in the 8-Å structure of the CP47 RC (*12*). The assignment of a CP43 Chl cannot be ruled out from the CP47 RC structure, but a CP43 orientation symmetric to CP47 would also put the closest CP43 Chl a significant distance away from Q_A. Assuming homology to the BRC and based on distance alone, Chl_Z and Chl_D are the least likely of the RC Chls to be affected by Q_A^-: the homologues of the amino acids that ligate Chl_Z/Chl_D are 32.8/42.0 Å from MQ (Table 3). Furthermore, mutants in which the Chl_Z/Chl_D axial ligands are perturbed (D1-H118Q/D2-H117Q) do not show a difference in their Q_A^- minus Q_A spectra relative to WT (Figure 5). Similarly, the absence of a shifting band at 672 nm in the D1-H198Q Q_A^- minus Q_A spectrum rules out P_A as a candidate. Because P_B is expected to be in close proximity to P_A and to have a similar distance with respect to Q_A, it seems unlikely that P_B is the fourth chromophore affected by Q_A reduction. In the BRC, the remaining RC BChl, the M-branch voyeur BChl, is slightly farther from MQ than the special pair BChls; thus, B_B does not appear to be ideally situated for interaction with Q_A^-. On the other hand, a distance between B_B (and B_A) and Q_A predicted based on the BRC structure may be flawed given that the axial ligands of the voyeur BChls are not conserved in PSII (*9*). A difference in the positions of the voyeur BChls and B_A/B_B relative to the quinones (*23*) could result in a stronger B_B-Q_A^- interaction in PSII. One factor favoring the assignment of B_B as the fourth chromophore shifted by Q_A reduction is the fact that it supports a model of the RC in which symmetry plays a significant role: the four chromophores shifted by Q_A reduction would be both Pheos, B_A, and B_B, with each pair related by 2-fold symmetry. We tentatively assign B_B as the second Chl shifted by Q_A reduction.

In general, the chromophore assignments are consistent with a structure of the PSII RC that is similar to that of the BRC. For example, the dominant band shift contributing to the Q_A^- minus Q_A spectrum corresponds to Pheo(D1), the chromophore which is expected to be the closest to Q_A and the most strongly influenced by Q_A reduction based on the BRC structure (Table 3). Similarly, the band shift of Pheo(D2) has a significant contribution to the Q_A^- minus Q_A spectrum, and the homologous BPheo is the second closest chromophore to MQ in the BRC. B_A is also influenced by Q_A reduction, and its homolog, the L-branch voyeur BChl, is the third closest chromophore to MQ. The absence of an influence of Q_A^- on P_A revealed using the D1-H198Q mutant is consistent with a position relative to Q_A that is similar to that found between the L-branch special pair Chl and MQ: the large distance relative to MQ predicts a weak electrochromic interaction between P_A and Q_A. Also, the band shift direction observed for three of the four PSII chromophores agrees with that predicted based on the orientation of BRC chromophores (Table 3).

Despite the consistencies between the BRC structure and the observed band shifts in PSII, there are some differences that indicate variation between the different types of reaction centers. A comparison of MQ^- minus MQ spectra for the BRC (*45, 46*) with the Q_A^- minus Q_A spectrum reveals that the dominant band shifts in the two spectra have opposite directionality: the main band shift in PSII is a blue shift of Pheo(D1) while the dominant band shift in the BRC is a red shift of one or both of the BPheos. Interestingly, the Q_x region band shift corresponding to Pheo(D1) is a blue shift, but the Q_x band shift for Pheo(D2) is a red shift (Force, D. A., and Diner, B. A., unpublished results). Thus, the shift directionalities in the Q_x and Q_y regions are the same for a given Pheo within PSII. Another difference between PSII and the BRC is that, in the MQ^- minus MQ spectrum, band shifts from the special pair BChls contribute more to the spectrum than band shifts of the voyeur BChls (*45, 46*). This is in contrast to our assignments for PSII in which B_A and B_B contribute to the Q_A^- minus Q_A spectrum and P_A and P_B do not contribute significantly.

There are several factors that may explain the spectral differences between PSII and the BRC. One possibility is that the orientations of the chromophores diverge between the BRC and PSII, an interpretation that has been applied before to the Pheos and Q_A in PSII (*20*, *23*). Such variations would change the orientation of chromophore Q_y transition dipoles with respect to Q_A^-, giving rise to band shifts with different intensities or directionality relative to the BRC. This influence may contribute to the different responses of P_A and the L-branch special pair BChl to Q_A/MQ reduction because P_A and P_B are known to have a different position than the special pair BChls (*12*), and a different orientation is likely (*12*, *23*). Another possibility is that the Q_y transition dipoles for the PSII Chls are different from those of the BRC BChls (*19*). If this is true, then the distribution of electron density within the chlorin rings in the ground and excited states would be different in PSII versus the BRC and would lead to different sensitivities of the chromophores to nearby charged species. In addition, local differences in the dielectric constant of the protein medium are likely to contribute because changes in dielectric strength modulate the magnitude of electrochromic band shifts. In fact, it has been shown that the active and inactive BPheo branches in the BRC display significant asymmetry: the effective dielectric constant along the L-branch of the BRC is significantly higher than that of the M-branch, resulting in smaller electrochromic shifts of the L-branch chromophores (*47*). Combined with a different position for B_B than the M-branch voyeur BChl (see above), a low dielectric between B_B and Q_A could explain the significant shift of the B_B Q_y absorbance band upon Q_A reduction.

While Q_A^- minus Q_A spectra for WT and D1-Q130E were fit and explained best using a blue-shifting Pheo(D1) as described in detail above, the spectra could be fit reasonably well by using a red-shifting Pheo(D1) model. However, this latter model is not favored because it requires a large difference between the band shift magnitudes for Pheo(D1) in WT versus D1-Q130E. Such variation is difficult to justify given the subtle nature of the D1-Q130E mutation and the fact that WT and D1-Q130E show Q_x band shifts that are

very similar in magnitude. In addition, the red-shifting Pheo(D1) model required a weak interaction between Pheo(D1) and Q_A^-, an unlikely scenario given their expected close proximity.

Comparison to Previous Assignments. In the presence of neutral Q_A, the two Pheos have absorbance maxima at 669.3 and 685.6 nm. These positions are consistent with previous assignments. The photochemically inactive Pheo molecule was estimated to absorb at 671 ± 1 nm (*22*), and other groups have suggested that one of the Pheos in PSII absorbs at about 670 nm (*24, 25, 48, 49*). The photochemically active Pheo has been assigned to be in the range of wavelengths between 680 and 685 nm (*2, 20, 22, 23, 50*−*52*), so our assignment is at the upper end of this range.

Despite the general agreement between our assignments and others, there are several factors that may explain why some previous studies have differed. One issue is the impact of sample preparation on spectral assignment. In fact, this has been presented as an explanation for the wide range of absorbance band assignments obtained from D1/D2/cyt b_{559} preparations (*20*). The detergent treatments used to prepare these stripped-down complexes by removing antenna proteins may have a significant impact on the absorbance bands of the core chromophores by perturbing the chromophore environment within the protein. There is evidence of a 4−5-nm blue shift of P680 upon conversion from intact PSII to isolated D1/D2/cyt b_{559} complexes, and it has been suggested that the low-energy (∼684 nm) bands contributing to D1/D2/cyt b_{559} spectra may actually represent the residual fraction of centers that remain as intact PSII (*20*). Similarly, the Q_y band of P680 may be perturbed by the harsh chemical treatment used to produce doubly reduced Q_A (*20*). These arguments reinforce the importance of considering the individual PSII preparation and treatment used for chromophore assignments. The PSII core complexes used in this work consist of the RC complex plus additional associated proteins. In these preparations, the CP43 and CP47 proteins are likely to have a role in stabilizing the RC and preserving the native protein environment of RC core chromophores.

In some previous assignments of electrochromic spectra, there have been simplifying assumptions about the number and λ_{max} of chromophores contributing to various spectra. For example, in one study of electrochromic band shifts of PSII it was assumed that a total of four chromophores are influenced by redox changes on Q_A, Y_Z, and the Mn cluster (*23*). While these assumptions rendered the spectral fits tractable, they de-emphasized the expected symmetry of the D1 and D2 Pheos and are not consistent with our finding that both Pheos are influenced by a redox change at Q_A. Similarly, a Q_A^- minus Q_A spectrum obtained by Velthuys which displays remarkable similarity to the WT Q_A^- minus Q_A spectrum presented here was simulated with only one Chl and one Pheo absorbance band (*53*). In light of the observations of this paper, the assignment of only two chromophores affected by Q_A reduction is certainly an underestimation. In other studies, some chromophore positions have been restricted to ranges of previously determined values (*24*). Again, this approach decreases the number of variables in fits but limits the independence of assignments from previous work. In this study, we have avoided assumptions about the contributing chromophores prior to the identification of absorbance bands from spectral fits.

Some groups have used the directionality of Q_A^--induced electrochromic shifts to argue in favor of or against similar placement of the Pheos and BPheos relative to Q_A in PSII and the BRC (*23, 54*). However, most descriptions of Q_A^- minus Q_A difference spectra report only one or two electrochromic shifts (*20, 21, 23, 38, 39, 45, 46, 54*). The data presented here show that Q_A reduction induces both blue and red shifts, and it is clear that a charge on Q_A alters the absorbance bands of more than one chromophore in PSII. Therefore, it is important to identify all of the affected chromophores and to consider the known chromophore stoichiometry differences between the complexes when evaluating the structural implications of spectral band shifts.

The identification of B_A at 683.5 nm is an assignment that has little basis for comparison because most efforts to identify RC chromophore bands have focused on the P680 Chls, the Pheos and the accessory Chls ligated by D1-H118 and D2-H117. However, efforts to assign low energy bands (682−684 nm) have been quite common, so several comments are warranted. Our assignment of B_A is in reasonable agreement with the work of Konermann et al., which simulated the temperature dependence of the RC Q_y spectrum and proposed an accessory Chl at 682.3 nm at 10 K (*24, 55*). On the other hand, the B_A assignment is in contrast to studies of detergent-treated PSII, which suggest that a 684 nm band corresponds to a labile Chl at the exterior of the RC (*26*) or Chl_Z (*56*), and it differs from studies which suggest that long wavelength (∼683 nm) Chls in some D1/D2/cyt b_{559} preparations represent contaminating antenna Chls that were not completely removed during the PSII isolation procedure (*24*). While our results do not exclude the possibility that more than one Chl in the RC absorbs at ∼684 nm, they do show that if only one Chl in the RC absorbs at ∼684 nm it can be assigned to B_A.

The absorbance bands and cofactor interactions assigned in this paper have implications for previous interpretations of PSII structure and chromophore orientations. In general, this work supports a structural model of PSII that is similar to the BRC. In particular, it appears that there are voyeur-like accessory Chls in PSII that are not Chl_Z or Chl_D, an assessment that is consistent with the consensus that there are six rather than four Chls per D1/D2/cyt b_{559} complex (*3*−*6, 56*). This work, therefore, strengthens the assignment of monomeric accessory Chls in the 8-Å structure of PSII that correspond to the monomeric BChls of the BRC, although their positions and/or orientations in PSII may be slightly different from those in the BRC. Also, the observation that Chl_Z and Chl_D are not influenced by the redox state of Q_A supports the model of cyclic electron transfer in PSII in which the electron acceptor (Q_A) and donor (Chl_Z) sides are separated by more than one electron-transfer step and are bridged by the redox-active mediator, cyt b_{559} (*57*−*59*). The identification of an effect on both Pheos, B_A, and another Chl in PSII due to the charge on Q_A demonstrates the sensitivity of the PSII absorbance profile to redox changes and electron-transfer reactions within the RC.

FUTURE PERSPECTIVES

The survey of redox-induced spectral features presented here demonstrates that there is a significant amount of structural and spectroscopic information to be obtained by

the application of optical difference spectroscopy to site-directed mutants of PSII. Despite extensive study, none of the Q_y absorbance bands of Chls and Pheos in PSII had been unambiguously assigned, and LT optical spectroscopy of various redox states provides a means of assigning some of these components. The application of this technique to the many existing site-directed mutants of PSII—especially mutants in which the binding environments of RC chromophores are perturbed—will enable the assignment of all of the chromophores and provide important insights into the interactions between the cofactors in PSII.

The case presented in this paper is limited to providing information about chromophores whose absorbance bands are influenced by the redox state of Q_A, but the approach utilized is shown to be generally very useful for assigning individual absorbance bands that are part of a complex group of overlapping bands. This strategy will certainly be productive in the future to examine difference spectra of other redox states such as $Y_Z^{\bullet}$ minus Y_Z, $Y_D^{\bullet}$ minus Y_D, Q_B^- minus Q_B, Chl_Z^+ minus Chl_Z, and Car^+ minus Car in conjunction with site-directed mutants and our ever-increasing structural insight to elucidate the absorbance profile of PSII.

ACKNOWLEDGMENT

We thank Dr. John Hartwig for the loan of the Lambda 6 UV−Vis spectrophotometer. D.H.S. thanks Dr. Veronika Szalai for many useful discussions and for critical reading of the manuscript.

REFERENCES

1. Tang, X.-S., and Satoh, K. (1985) *FEBS Lett. 179*, 60−64.
2. Nanba, O., and Satoh, K. (1987) *Proc. Natl. Acad. Sci. U.S.A. 84*, 109−112.
3. Gounaris, K., Chapman, D. J., Booth, P. J., Crystall, B., Giorgi, L. B., Klug, D. R., Porter, G., and Barber, J. (1990) *FEBS Lett. 265*, 88−92.
4. Kobayashi, M., Maeda, H., Watanabe, T., Nakane, H., and Satoh, K. (1990) *FEBS Lett. 260*, 138−140.
5. Eijckelhoff, C., Van Roon, H., Groot, M.-L., Van Grondelle, R., and Dekker, J. P. (1996) *Biochemistry 35*, 12864−12872.
6. Tomo, T., Mimuro, M., Iwaki, M., Kobayashi, M., Itoh, S., and Satoh, K. (1997) *Biochim. Biophys. Acta 1321*, 21−30.
7. Hankamer, B., Barber, J., and Boekema, E. J. (1997) *Annu. Rev. Plant Physiol. Plant Mol. Biol. 48*, 641−671.
8. Debus, R. J. (1992) *Biochim. Biophys. Acta 1102*, 269−352.
9. Michel, H., and Deisenhofer, J. (1988) *Biochemistry 27*, 1−7.
10. Ruffle, S. V., Donnelly, D., Blundell, T. L., and Nugent, J. H. A. (1992) *Photosynth. Res. 34*, 287−300.
11. Svensson, B., Etchebest, C., Tuffery, P., van Kan, P., Smith, J., and Styring, S. (1996) *Biochemistry 35*, 14486-14502.
12. Rhee, K.-H., Morris, E. P., Barber, J., and Kühlbrandt, W. (1998) *Nature 396*, 283−286.
13. Koulougliotis, D., Tang, X.-S., Diner, B. A., and Brudvig, G. W. (1995) *Biochemistry 34*, 2850−2856.
14. Stewart, D. H., Cua, A., Chisholm, D. A., Diner, B. A., Bocian, D. F., and Brudvig, G. W. (1998) *Biochemistry 37*, 10040−10046.
15. Diner, B. A., Nixon, P. J., and Farchaus, J. W. (1991) *Curr. Opin. Struct. Biol. 1*, 546−554.
16. El-Kabbani, O., Chang, C.-H., Tiede, D., Norris, J., and Schiffer, M. (1991) *Biochemistry 30*, 5361−5369.
17. Diner, B. A., and Babcock, G. T. (1996) in *Advances in Photosynthesis* (Ort, D. R., and Yocum, C. F., Eds.) pp 213−247, Kluwer Academic Publishers, Dordrecht.
18. Tommos, C., Hoganson, C. W., Di Valentin, M., Lydakis-Simantiris, N., Dorlet, P., Westphal, K., Chu, H.-A., McCracken, J., and Babcock, G. T. (1998) *Curr. Opin. Chem. Biol. 2*, 244−252.
19. Hanson, L. K., Fajer, J., Thompson, M. A., and Zerner, M. C. (1987) *J. Am. Chem. Soc. 109*, 4728−4730.
20. Hillmann, B., Brettel, K., van Mieghem, F., Kamlowski, A., Rutherford, A. W., and Schlodder, E. (1995) *Biochemistry 34*, 4814−4827.
21. Hillmann, B., and Schlodder, E. (1995) *Biochim. Biophys. Acta 1231*, 76−88.
22. Mimuro, M., Tomo, T., Nishimura, Y., Yamazaki, I., and Satoh, K. (1995) *Biochim. Biophys. Acta 1232*, 81−88.
23. Mulkidjanian, A. Y., Cherepanov, D. A., Haumann, M., and Junge, W. (1996) *Biochemistry 35*, 3093−3107.
24. Konermann, L., and Holzwarth, A. R. (1996) *Biochemistry 35*, 829−842.
25. Braun, P., Greenberg, B. M., and Scherz, A. (1990) *Biochemistry 29*, 10376−10387.
26. Chang, H.-C., Jankowiak, R., Reddy, N. R. S., Yocum, C. F., Picorel, R., Seibert, M., and Small, G. J. (1994) *J. Phys. Chem. 98*, 7725−7735.
27. Williams, J. G. K. (1988) *Methods Enzymol. 167*, 766−778.
28. Giorgi, L. B., Nixon, P. J., Merry, S. A. P., Joseph, D. M., Durrant, J. R., De Las Rivas, J., Barber, J., Porter, G., and Klug, D. R. (1996) *J. Biol. Chem. 271*, 2093-2101.
29. Nixon, P. J., Trost, J. T., and Diner, B. A. (1992) *Biochemistry 31*, 10859−10871.
30. Tang, X.-S., and Diner, B. A. (1994) *Biochemistry 33*, 4594−4603.
31. Tamura, N., and Cheniae, G. (1987) *Biochim. Biophys. Acta 890*, 179−194.
32. Lichtenthaler, H. K. (1987) *Methods Enzymol. 148*, 350−382.
33. Metz, J. G., Nixon, P. J., Rögner, M., Brudvig, G. W., and Diner, B. A. (1989) *Biochemistry 28*, 6960−6969.
34. Shipman, L. L. (1982) in *Photosynthesis* (Govindjee, Ed.) pp 275−291, Academic Press, New York.
35. Giuffra, E., Zucchelli, G., Sandonà, D., Croce, R., Cugini, D., Garlaschi, F. M., Bassi, R., and Jennings, R. C. (1997) *Biochemistry 36*, 12984−12993.
36. Simonetto, R., Crimi, M., Sandonà, D., Croce, R., Cinque, G., Breton, J., and Bassi, R. (1999) *Biochemistry 38*, 12974−12983.
37. Babcock, G. T., Ghanotakis, D. F., Ke, B., and Diner, B. A. (1983) *Biochim. Biophys. Acta 723*, 276−286.
38. van Gorkom, H. J., Tamminga, J. J., and Haveman, J. (1974) *Biochim. Biophys. Acta 347*, 417−438.
39. van Gorkom, H. J. (1974) *Biochim. Biophys. Acta 347*, 439−442.
40. Miller, A.-F., and Brudvig, G. W. (1991) *Biochim. Biophys. Acta 1056*, 1−18.
41. Bylina, E. J., Kirmaier, C., McDowell, L., Holten, D., and Youvan, D. C. (1988) *Nature 336*, 182−184.
42. van Kan, P. J. M., Otte, S. C. M., Kleinherenbrink, A. M., Nieveen, M. C., Aartsma, T. J., and van Gorkom, H. J. (1990) *Biochim. Biophys. Acta 1020*, 146−152.
43. Zucchelli, G., Garlaschi, F. M., and Jennings, R. C. (1996) *Biochemistry 35*, 16247−16254.
44. Deisenhofer, J., Epp, O., Miki, K., Huber, R., and Michel, H. (1985) *Nature 318*, 618−624.
45. Vermeglio, A., and Clayton, R. K. (1977) *Biochim. Biophys. Acta 461*, 159−165.
46. Shopes, R. J., and Wraight, C. A. (1985) *Biochim. Biophys. Acta 806*, 348−356.
47. Steffen, M. A., Lao, K., and Boxer, S. G. (1994) *Science 264*, 810−816.
48. Klimov, V. V., Klevanik, A. V., Shuvalov, V. A., and Krasnovsky, A. A. (1977) *FEBS Lett. 82*, 183−186.
49. Shuvalov, V. A., Heber, U., and Schreiber, U. (1989) *FEBS Lett. 258*, 27−31.
50. Ganago, I. B., Klimov, V. V., Ganago, A. O., Shuvalov, V. A., and Erokhin, Y. E. (1982) *FEBS Lett. 140*, 127−130.
51. Tang, D., Jankowiak, R., Seibert, M., Yocum, C. F., and Small, G. J. (1990) *J. Phys. Chem. 94*, 6519−6522.
52. van der Vos, R., van Leewen, P. J., Braun, P., and Hoff, A. J. (1992) *Biochim. Biophys. Acta 1140*, 184−198.

53. Velthuys, B. R. (1988) *Biochim. Biophys. Acta 933*, 249−257.
54. Cherepanov, D. A., Haumann, M., Junge, W., and Mulkidjanian, A. (1995) in *Photosynthesis: from Light to Biosphere* (Mathis, P., Ed.) pp 531−534, Kluwer Academic Publishers, Dordrecht.
55. Konermann, L., Yruela, I., and Holzwarth, A. R. (1997) *Biochemistry 36*, 7498−7502.
56. Jankowiak, R., Rätsep, M., Picorel, R., Seibert, M., and Small, G. J. (1999) *J. Phys. Chem. B 103*, 9759−9769.
57. Thompson, L. K., and Brudvig, G. W. (1988) *Biochemistry 27*, 6653−6658.
58. Stewart, D. H., and Brudvig, G. W. (1998) in *Photosynthesis: Mechanisms and Effects* (Garab, G., Ed.) pp 1113−1116, Kluwer Academic Publishers, Dordrecht.
59. Stewart, D. H., and Brudvig, G. W. (1998) *Biochim. Biophys. Acta 1367*, 63−87.

BI001246J